LDV measurements of the velocity field on the inlet section of a pumped storage equipped with a symmetrical suction elbow for variable discharge values

I Drăghici[1], S Muntean[2], A I Bosioc[1] and L E Anton[1]
[1] Department of Hydraulic Machinery, University Politehnica Timisoara, Bv. Mihai Viteazu, No. 1, Ro-300222, Timisoara, Romania
[2] Center for Advanced Research in Engineering Sciences, Romanian Academy – Timisoara Branch, Bv. Mihai Viteazu, No. 24, Ro-300223, Timisoara, Romania

E-mail: seby@acad-tim.tm.edu.ro

Abstract. The storage pumps are equipped with various types of inlet casings. The flow non-uniformity is generated by the suction elbows being ingested by the impeller leading to unsteady phenomena and worse cavitational behaviour. A symmetrical suction elbow model corresponding to the double flux storage pump was manufactured and installed on the test rig in order to assess the flow field at the pump inlet. The experimental investigations are performed for 9 discharge values from 0.5 to 1.3 of nominal discharge. LDV measurements are performed on the annular section of the pump inlet in order to quantify the flow non-uniformity generated by the symmetrical suction elbow. Both axial and circumferential velocity components are simultaneously measured on the half plane (180°) of the annular inlet section along to 19 survey axis with 62 points on each. The flow field on the next half plane is determined tacking into account the symmetry. As a result, the flow map on the pump inlet annular section is reconstructed revealing a significant variation of the circumferential velocity component. The absolute flow angle is computed showing a significant variation of ±38°.

1. Introduction

The large pumping units are widely used in industry to store energy, to provide cooling, to ensure propulsion and to transfer fluids. These pumps can reach high values of flow rate at high efficiency with a tolerate level of cavitation behaviour if its selection criteria with respect to suction behaviour and optimum efficiency meet various system requirements [1]. The large pumping units consume a significant amount of the electrical energy. Therefore, even smaller improvements of energetical and cavitational performances of the large pumps are significant to minimize the overall costs.

Three pumped storage power plants (PSPP) are integrated in one of the most complex hydropower system from Romania located on the Lotru river, Cojocar [2]. PSPP considered like test case is equipped with two units. Each unit includes synchronous electrical motor (blue), elastic coupling (yellow) and double flux pumped storage (green) like in Fig. 1. The unit was designed in order to deliver large flow rate at high efficiency operating under tolerant cavitation conditions. In situ measurements were performed after 25 years of operation in order to evaluate the unit performances, Anton [3]. A worse cavitational behaviour was revealed in service. The same problems were reported by Škerlavaj et al. [4] in operation of the units from Fuhren HPP.

The paper investigates the flow non-uniformity generated by a symmetrical suction elbow at the pump inlet for different discharges. The experimental test rig is described in Section 2. The setup for LDV measurements together with experimental details are presented in Section 3. The experimental data are shown and analyzed in Section 4. The conclusions are drawn in last section.

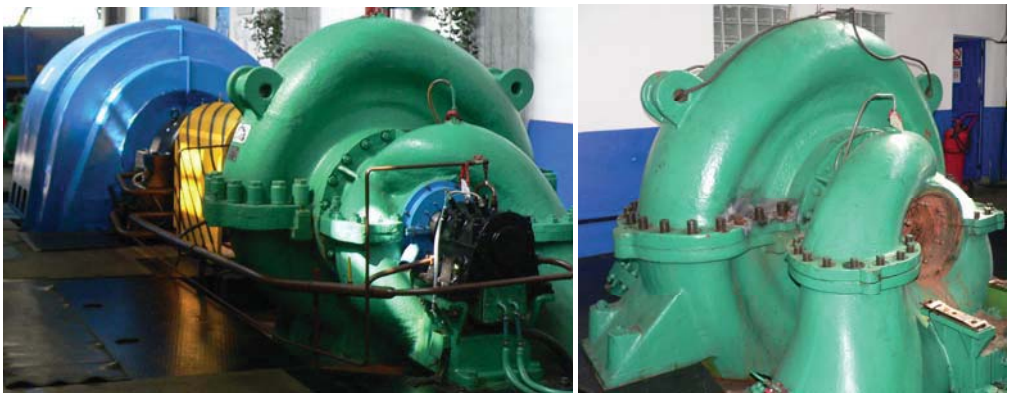

Fig. 1 Unit installed into the pumped storage power plant (left) and the double flux pump (right)

2. Experimental test rig

A test rig was developed at University Politehnica Timisoara in order to investigate the pump hydrodynamics, Fig. 2. It consists of two tanks of 1 m^3 each, a set of pipes and vanes, which form a closed hydraulic circuit, and a PCN 80-200 pump actuated by a 37 kW asynchronous motor. The inlet and outlet pipes diameters are 0.1 m and 0.08 m, respectively. The pump parameters are presented in Table 1 while the energetical and cavitational curves are plotted in [5]. The characteristic speed of the pump impeller is n_q~30.

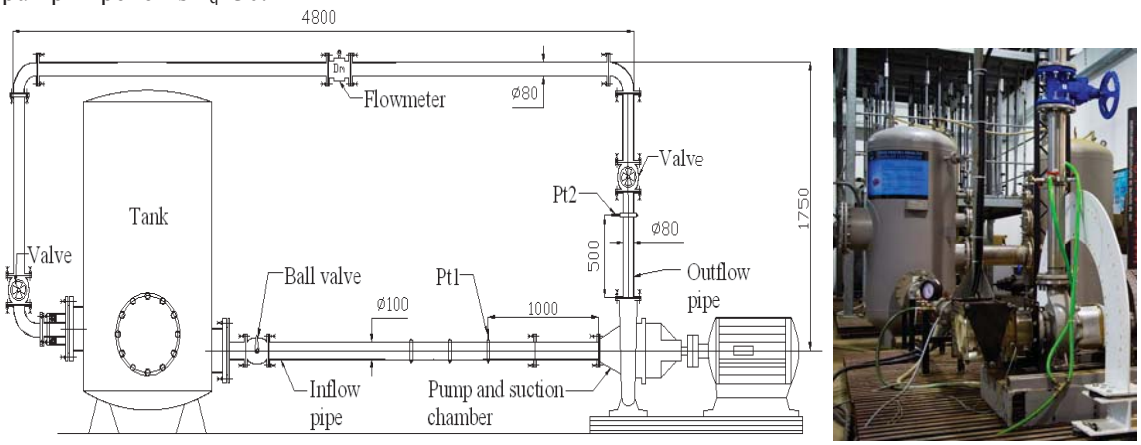

Fig. 2 Schematic view of the test rig with actual dimensions in mm (left) and photo (right).

Table 1. Hydraulic pump parameters.

Parameter	Value
Nominal speed n [rpm]	3000
Nominal puming head H_n [m]	44
Nominal discharge Q_n [m3/s]	0.0335
Power at nominal discharge P_n [kW]	20
Maximum efficiency [%]	72

The test rig is equipped with a real time acquisition data system. To acquire pressure at the inlet and outlet sections of the pump the rig is equipped with two pressure transducers: a vacuum gauge, located on the inlet pipe denoted Pt1 as well as a manometer placed on the outlet pipe labelled Pt2, in Fig. 2. An electromagnetic flow meter is installed on the rig`s top pipe in order to measure the discharge. Its range is 0÷45 l/sec with an accuracy reported to be ±0.4%. Real time data acquisition system ensures proper sensor biasing and serial PC communication.

3. LDV measurements setup

The inlet suction through which passes a pump shaft surrounded by a protective sleeve at least one radial rib is mounted on the sleeve surface away from the elbow inlet, [6]. In our case, two ribs are included like in Fig. 3. The rib R1 is located where the two partial flows around the hub meet. If this rib is omitted, cavitation characteristics and work transfer (head coefficient and efficiency) are seriously affected. A periodic pre-rotation can also be induced which would result in unsteady operating. The rib R2 is not absolutely necessary with symmetrical inlets but desirable for reasons of mechanical design in order to limit casing deformation under the internal pressure, [7].

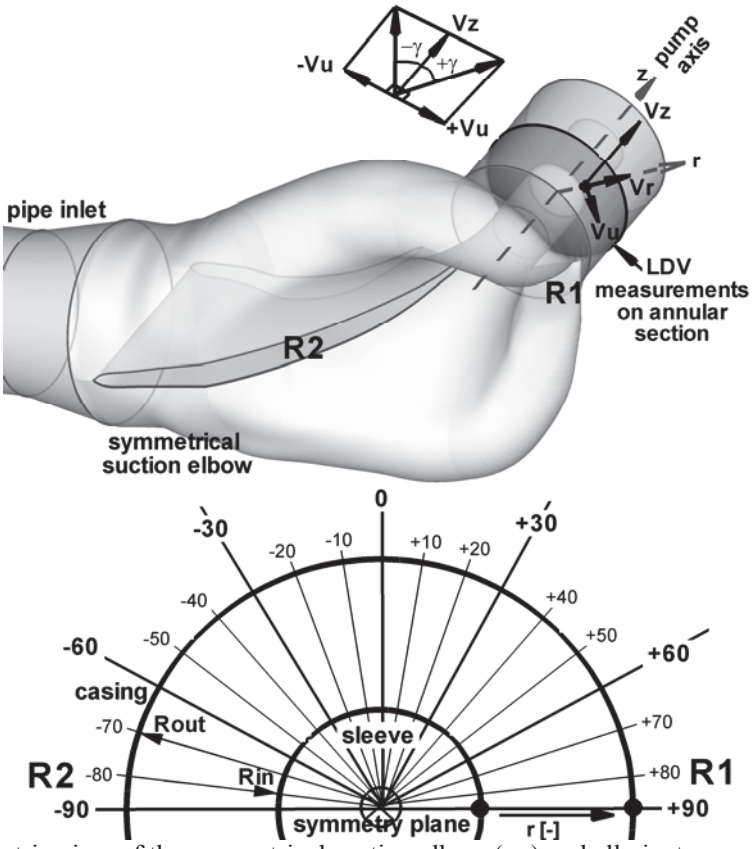

Fig. 3 Axonometric view of the symmetrical suction elbow (up) and all nineteen radial survey axes selected on the annular section for LDV investigations (down).

As it is previously mentioned, the flow with pre-rotation is generated in the symmetric inlet suction over roughly one half of the impeller inlet section and counter-rotation in the second half. The symmetry plane includes the rib R2 located at -90° and the rib R1 positioned at +90° like in Fig. 3. Therefore, the measurements are performed over upper half plane of the inlet section.

The three-dimensional complex shape of the suction elbow was milled out into the plexiglass brick in order to be visualized the flow field. An annular section is displaced between the elbow outlet and

the pump inlet, see Fig. 3. This annular section pump inlet is bounded by the sleeve shaft in the inner part with diameter of $D_{in}=2*R_{in}=40.2$ mm and the casing in the outer one with diameter of $D_{out}=2*R_{out}=103$ mm, respectively. The ratio between sleeve and casing diameters is 0.4. The optical window was installed on this cylindrical test section. Laser Doppler Velocimetry (LDV) measurements are performed along to the radial survey axis in 62 points with step of 0.5 mm. The annular test section is rotated around its axis in order to be measured on several radial survey axes. The measurements were done along to 19 radial survey axes from -90° to 90° with 10° increment, Fig 4. The laser probe curved link on the semi-circular support in order to be radial aligned with optical window on each survey axis position. Several alignments and checks were performed for the optical system on each radial survey axis position in order to be ensured uncertainties less than 2.5%. Each alignment procedure includes the following: the laser beams alignment, the cylindrical test section rotation around its axis and the optical window, respectively.

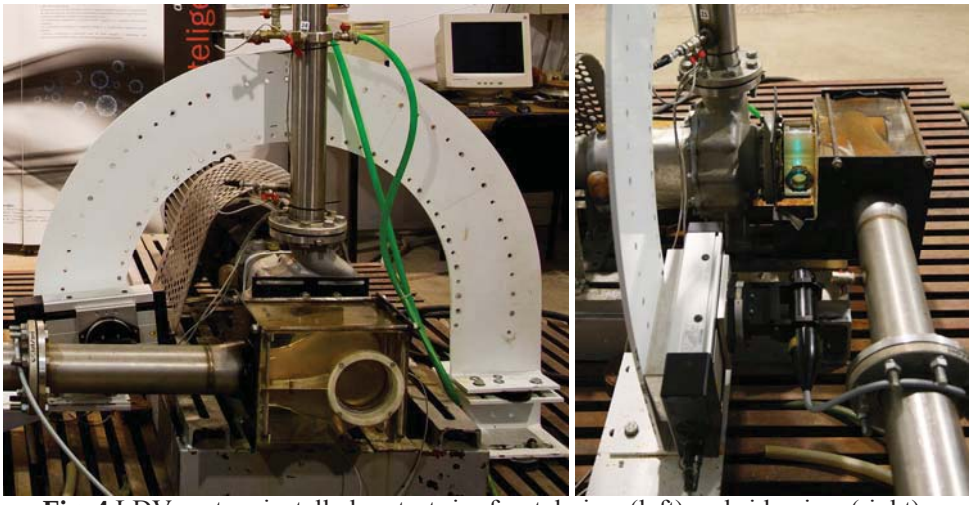

Fig. 4 LDV system installed on test rig: frontal view (left) and side view (right).

The experimental investigation was performed with a LDV system able to simultaneously measure two velocity components (axial and tangential components). LDV system measures the velocity of the seeds (silver coated particles with 10 μm diameter) inserted in the water. The measurements were performed with minimum 1000 samples/second (1 kHz sampling frequency). LDV system consists in an argon-ion source with 300 mW power and an optical fibber who guide the beams to the flow. The main characteristics of the LDV system are as follow: focal length of the probe 400 mm; beam diameter 2.2 mm; beam spacing 39.2 mm. For the probe positioning on radial survey axis, 1D traversing system is used with 0.01 mm accuracy. It was established that for each point is necessary to measure 50000 particles in 20 seconds in order to be ensured uncertainties less than 2.5%.

4. Experimental data

LDV measurements are performed along to nineteen radial survey axes (see Fig. 3) for nine discharge values from $0.5Q_n$ to $1.3Q_n$ with increment of $0.1Q_n$. The average absolute velocity profiles (V_z axial and V_u circumferential velocity components) versus radial coordinate were measured on all radial survey axes. Both dimensionless velocity components are obtained taking into account the average velocity value $V_m=Q/A$ according to the following equations:

$$v_z = \left(\frac{V_z}{Q/A} \right), \; v_u = \left(\frac{V_u}{Q/A} \right) \; [-] \tag{1}$$

where Q corresponds to the discharge value for each regime and the area A of the annular surface is computed as follow: $A=\pi(R_{out}^2-R_{in}^2)$.

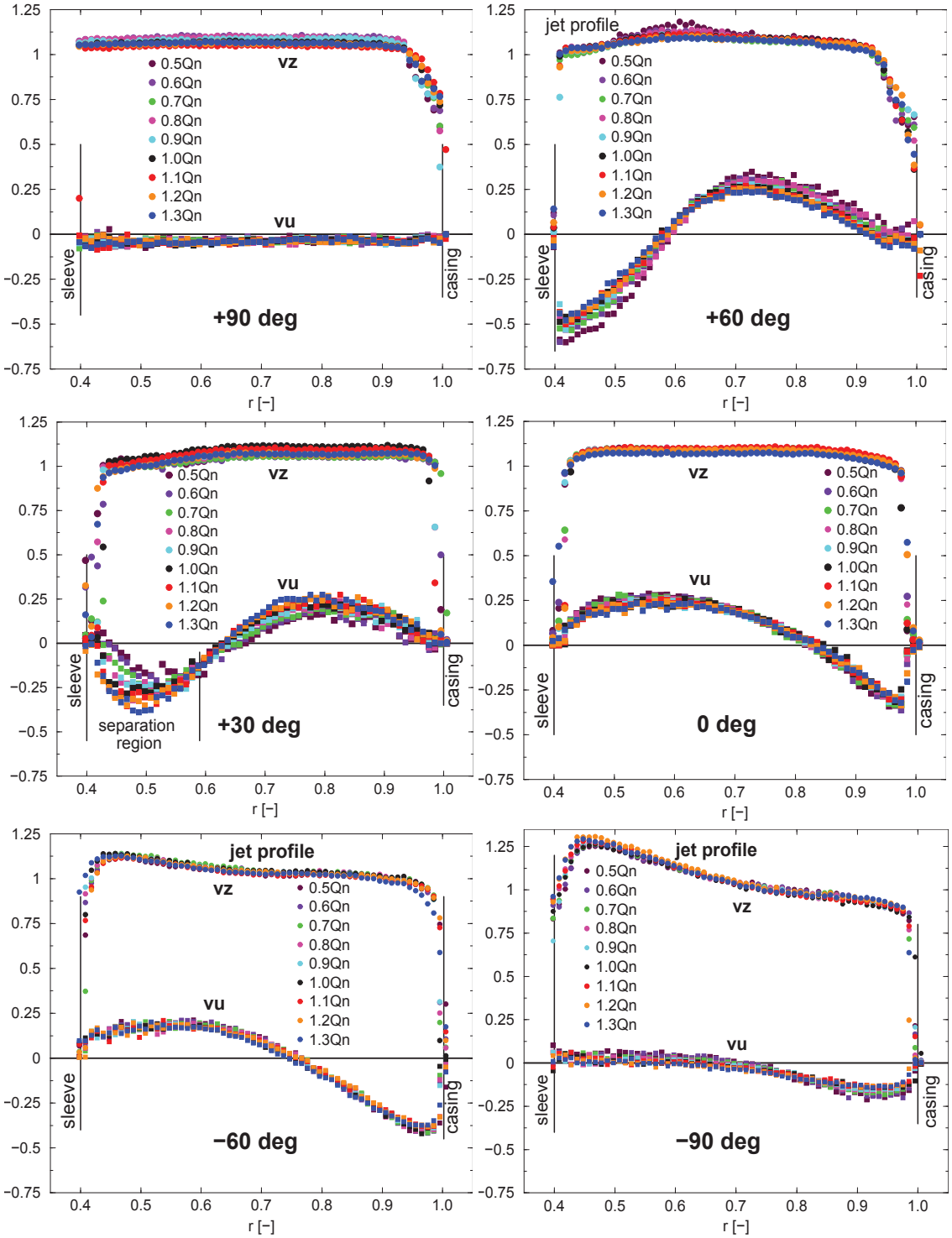

Fig. 5 Dimensionless averaged velocity components (v_z – axial and v_u – circumferential) measured along to six radial survey axes located at +90°, +60°, +30°, 0°, -60°, -90° on the annular surface.

The average dimensionless velocity profiles along to six radial survey axes are plotted in Fig. 5. One can observe that average dimensionless velocity profiles are discharge independent. However,

from +10° to +30° near to the sleeve is remarked a small variation of the circumferential velocity component with the discharge value. Also, a larger root mean square value is associated to each experimental point located in this separation region. Nevertheless, the average dimensionless absolute velocity profiles can be considered discharge independent even if the circumferential component of the velocity is slightly modified with the discharge value in this particular region.

The discharge value is computed based on LDV data using next equation in order to check the accuracy of the measurements:

$$Q_V = 2 \int_{-\pi/2}^{\pi/2} \int_{R_{in}}^{R_{out}} V_z(r,\theta)\, r\, dr\, d\theta \tag{2}$$

The relative error ε_r between the discharge value computed according to eq. (2) and the value measured with the flow meter is determined using eq. (3):

$$\varepsilon_r = \frac{Q_V - Q}{Q} 100 \ [\%] \tag{3}$$

A small relative error value equal to $\varepsilon_r = 0.49\%$ is obtained validating the velocity measurements.

Both maps of the dimensionless velocity components (axial v_z and circumferential v_u) measured on half of the annular surface are plotted in Fig. 6. One can observe a quasi-uniform distribution of the axial velocity component. However, two jets with larger dimensionless axial velocity then unit (the spots with light green colour) are identified while the smallest values of this component can be observed near to the walls. Contrary, the distribution of the circumferential velocity component is strongly non-uniform over one half of the annular section.

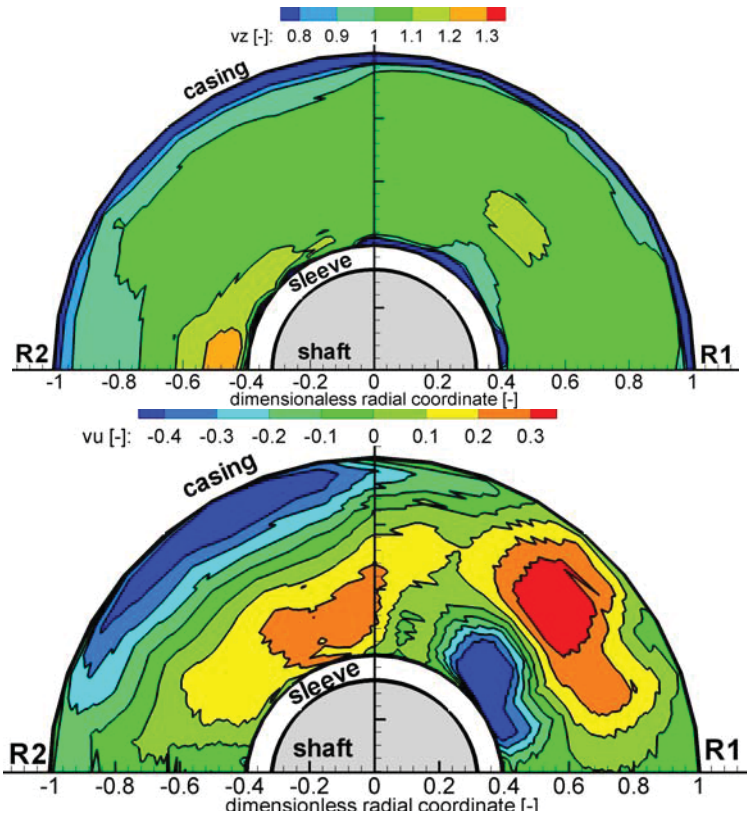

Fig. 6 Dimensionless velocity components maps measured on the half annular section: axial v_z (up) and circumferential v_u (down).

The flow angle γ is defined according to next equation in order to be quantified the deviation of the flow from the axial direction, see Fig. 3:

$$\gamma = arctg\left(\frac{V_u}{V_z}\right) \quad [^\circ] \tag{4}$$

The flow angle on seven radial survey axes is plotted in Fig. 7 while the map over full annular section is presented in Fig. 8. A strong non-uniformity of the flow angle is clearly revealed.

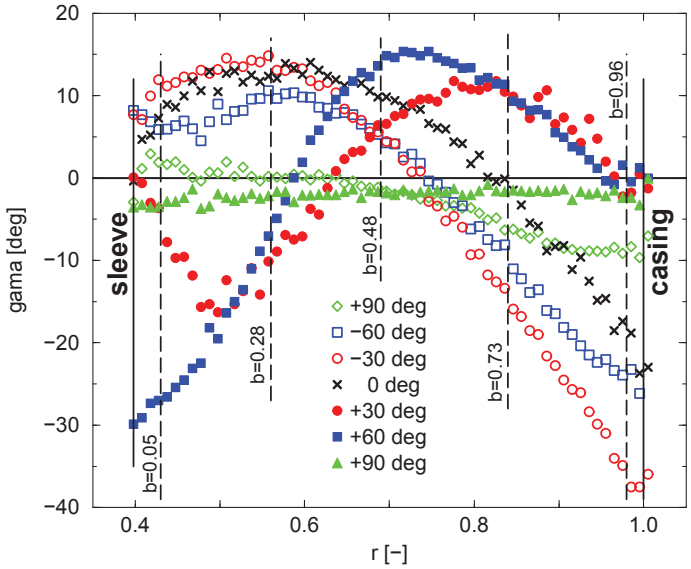

Fig. 7 Flow angle (γ) radial distribution on seven radial survey axes.

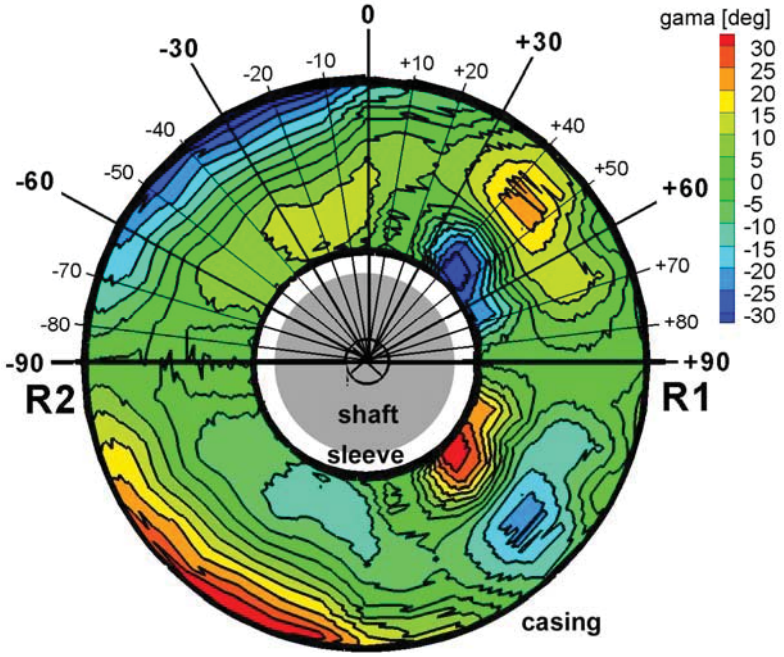

Fig. 8 Flow angle (γ) map on the annular section based on LDV measurements.

The most significant variation of the flow angle on the annular surface of the outlet suction elbow is generated near the boundaries (in vicinity of sleeve and casing, respectively), see Fig. 9. One can see that the largest flow non-uniformity of ±38° is measured near to the casing from -180° to 0°. However, a significant flow non-uniformity of ±33° is quantified near to the sleeve corresponding to the region from 0° to 180°. This non-uniform flow generated by the suction elbow is ingested by the impeller leading to the unwanted effects.

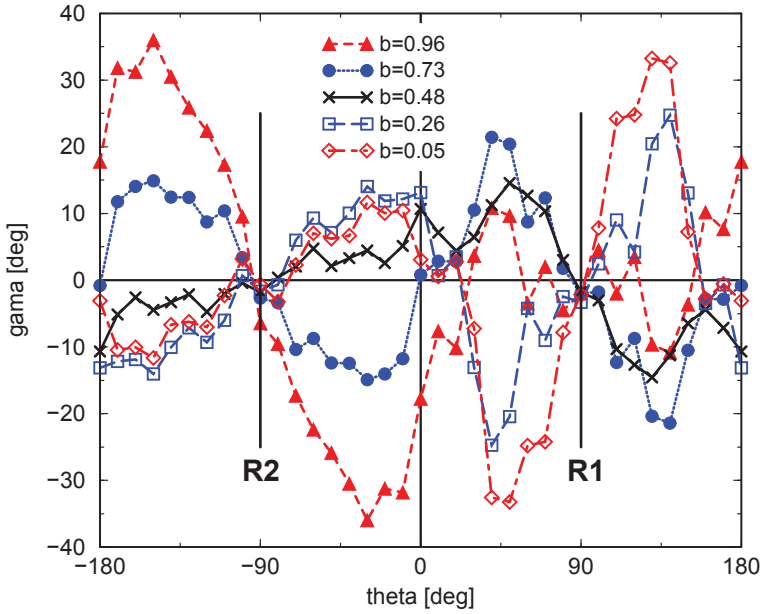

Fig. 9 Flow angle (γ) distribution along to five radii displaced on the annular section: b=0.05 (near to sleeve), 0.26, 0.48 (near to mid radius), 0.73, 0.96 (near to casing).

5. Conclusions

The paper experimentally investigates the non-uniform velocity field generated by three-dimensional complex geometry of the symmetrical suction elbow of the pumped storage. The non-uniform velocity field is measured with LDV system along to nineteen radial survey axes located at the outlet of the suction elbow for variable discharge values from 0.5Qn to 1.3Qn. The dimensionless averaged velocity field (axial and circumferential components) is obtained on a half annular section delimited by sleeve and casing, respectively. A quasi-uniform dimensionless axial velocity component is measured. Two jets with larger dimensionless axial velocity then unit are identified while the smallest values of this component is observed near to the walls. Contrary, the distribution of the circumferential velocity component is strongly non-uniform over one half of the annular section. From +10° to +30° near to the sleeve is remarked a small variation of the circumferential velocity component with the discharge value. Nevertheless, the average dimensionless velocity profiles can be considered discharge independent even if the circumferential component of the velocity is slightly modified with the discharge value in this particular region. The discharge value computed using the axial velocity component leads to a small relative error value equal to $\varepsilon_r = 0.49\%$ validating the velocity measurements.

The flow angle is determined based on both velocity components measured in order to quantify the deviation of the flow from the axial direction. The most significant variation of the flow angle on the annular surface of the outlet suction elbow is generated near the boundaries (in vicinity of sleeve and casing, respectively). One can see that the largest flow non-uniformity of ±38° is measured near to the

casing while a significant flow non-uniformity of ±33° near to the sleeve, respectively. A significant variation of the angle flow in front of the impeller is revealed. Consequently, the flow generated by the symmetrical suction elbow at the pump inlet is strongly non-uniform being far away from axial flow taken into account at the design stage. This non-uniform flow generated by the suction elbow is ingested by the impeller leading to the strong unwanted effects. Therefore, different solutions can be explored to improve the hydrodynamic conditions at pump inlet in order to reduce the maintenance cost and to extend the impeller lifetime [7 - 10].

Acknowledgements
This paper is supported by the Sectoral Operational Programme Human Resources Development POSDRU/159/1.5/S/137516 financed from the European Social Fund and by the Romanian Government. Dr. Muntean S. was supported by Romanian Academy program.

Nomenclature

Q_n [m^3/s]	nominal discharge
Q [m^3/s]	Discharge
Z, R, θ [m]	axial, radial and circumferential coordinates
V_z, V_r, V_u [m/s]	axial, radial and circumferential velocity components
v_z, v_r, v_u [-]	axial, radial and circumferential dimensionless velocity components
γ [°]	flow angle
ε_r [-]	relative error
A [m^2]	Area
R_{in}, R_{out} [m]	inner and outer radii
$b=(R-R_{in})/(R_{out}-R_{in})$ [-]	dimensionless distance between inner and outer radii

References

[1] Bolliger W and Leibundgut E 2004 Selection of Large Water Transport Pumps and Field Experiences, *in Proc. 21st Int. Pump Users Symposium*, (Collage Station, Texas), 48-61
[2] Cojocar M 2008 Hidroconstructia: Hydropower constructions, 2nd ed., **1**, (*Bucharest: Romania*).
[3] Anton A 2010 In situ performance curves measurements of large pumps, *IOP Conf. Ser.: Earth Environ. Sci.*, **12**, 012090:1-10
[4] Škerlavaj A, Titzschkau M, Pavlin R, Vehar F, Mežnar P and Lipej A 2012 Cavitation improvement of double suction centrifugal pump HPP Fuhren, *IOP Conf. Series: Earth and Environ. Sci.*, **15**, 022009:1 - 8
[5] Gînga G, Stanciu I R, Muntean S, Baya A and Anton LE 2012 3D Numerical Flow Analysis and Experimental Validation into a Model Impeller of a Storage Pump, *in Proc. Conf. Modelling Fluid Flow (CMFF'12)*, (Budapest, Hungary), **2**, 804 – 811
[6] Matthias H-B, Schramek W and Strscheletzly M 1968 Centrifugal Pump Inlet Elbow, US Patent No. 3411451
[7] Gülich J F 2010 Centrifugal Pumps, 2nd ed., (*Berlin: Springer Verlag*)
[8] Hergt P, Nicklas A, Mollenkopf G and Brodersen S 1996 The Suction Performance of Centrifugal Pumps Possibilities and Limits of Improvements, *in Proc. 13th Int. Pump Users Symposium*, (Collage Station, Texas), 13 - 26
[9] Ashihara K and Goto A 1999 Improvements of Pump Suction Performance using 3D Inverse Design Method, *in Proc. 3rd ASME/JSME Joint Fluids Engineering Conf. (FED99)*, (San Francisco, California), 1 - 12
[10] Moisă I G, Gînga G, Muntean S and Susan-Resiga R F 2012 Inverse Design and 3D Analysis of the Inducer for Storage Pump Impeller, *in Proc. Conf. Modelling Fluid Flow (CMFF'12)*, (Budapest, Hungary), **2**, 812 – 819